Investigation of multiple metal nanoparticles near-field coupling on the surface by discrete dipole approximation method*

YIN Ping (尹萍)[1], **LIN Qiang** (林强)[1], **RUAN Yi** (阮义)[1]**, **and CHEN Jing-jing** (陈菁菁)[2,3]

1. Zhejiang Provincial Key Laboratory & Collaborative Innovation Center for Quantum Precision Measurement, College of Science, Zhejiang University of Technology, Hangzhou 310023, China

2. College of Computer Science and Technology, Zhejiang University, Hangzhou 310001, China

3. College of Zhijiang, Zhejiang University of Technology, Shaoxing 312000, China

(Received 11 April 2020; Revised 16 June 2020)

We use the method of discrete dipole approximation with surface interaction to construct a model in which a plurality of nanoparticles is arranged on the surface of BK7 glass. Nanoparticles are in air medium illuminated by evanescent wave generated from total internal reflection. The effects of the wavelength, the polarization of the incident wave, the number of nanoparticles and the spacing of multiple nanoparticles on the field enhancement and extinction efficiency are calculated by our model. Our work could pave the way to improve the field enhancement of multiple nanoparticles systems.

Document code: A **Article ID:** 1673-1905(2021)05-0257-5

DOI https://doi.org/10.1007/s11801-021-0064-z

Total internal reflection occurs when a plane wave propagates from a medium of higher refractive index to a medium of lower refractive index with an incident angle exceeds the critical angle. Evanescent field, which is associated with total internal reflection, is generated in the vicinity of the boundary of two media[1]. The mean free path of electrons in general metals is smaller than the noble metals, the free electrons in the noble metal (Au/Ag/Cu) have a mean free path of about 50 nm[2]. In other words, noble metal nanoparticles have significant scattering phenomenon when excited. Placing noble metal nanoparticles with a diameter far less than the wavelength of the incident wave in the vicinity of surface, intensely absorption and scattering phenomena occurs, that is well known as localized surface plasmon resonance (LSPR) scattering[3]. Taking advantages of the strong LSPR scattering of noble metal nanoparticles, multiple-nanoparticles have great potential for application as catalysts, optics and biosensing[3-8]. For example, biomedical processes are also closely related to plasmon resonance in nanoparticles, such as Raman spectroscopy of analytes, fluorescence enhancement, catalysis, and conversion of sunlight energy in photosynthesis[9-12]. In addition, in the field of materials science, multi-nanoparticles are able to create new types of sensing materials with high sensitivity[13,14]. In nanoscience, multi-nanoparticles systems are widely used in studying nanodimer structures[7,15-17].

In this work, we used the discrete dipole approximation (DDA) method to simulate Ag nanoparticles (ANPs) Ag nanospheres disposed on the surface of BK7 glass, in the air medium[5,18-20], Nanoparticles are illuminated by evanescent wave generated from total internal reflection, the near-field coupling between multiple metal nanoparticles are calculated by DDA method[21-23]. It is worth noting that in our simulation, the arrangement of nanoparticles is approximately random, which is more in line with the actual condition of the experiment[24]. We discussed the effects of the wavelength, the polarization of the incident wave, the size and the number of ANPs and the spacing of multiple ANPs on the near-field coupling to optimize the experiment conditions.

In the DDA model, the arbitrary scattering object is considered as an array of point dipoles that interacts with the incident field[1]. In details, scattering object is discretized as point dipoles at position $\boldsymbol{r}_i$ (i=1,2,…,N) with polarizability α_i, where α_i is the Clausius-Mossotti polarizability[25]:

$$\alpha_i = \frac{3d^3}{4\pi}\left(\frac{\epsilon_i - 1}{\epsilon_i + 2}\right). \tag{1}$$

Assume $\boldsymbol{E}_i$ is the local field intensity of dipole at position $\boldsymbol{r}_i$, $\boldsymbol{E}_{\mathrm{inc},i}$ is the incident field which is equal to the sum of $\boldsymbol{E}_i$ plus contributions from the $N-1$ dipoles,

$$\boldsymbol{E}_{\mathrm{inc},i} = \boldsymbol{E}_i + \Sigma_{i\neq k}\boldsymbol{A}_{ik}\boldsymbol{P}_i, \tag{2}$$

and each point dipole at position $\boldsymbol{r}_i$ has polarization $\boldsymbol{P}_i$,

* This work has been supported by the Zhejiang Provincial Natural Science Foundation of China (No.LGF20C050001), and the National Nature Science Foundation of China (No.61805213).

** E-mail: yiruan@zjut.edu.cn

$$\boldsymbol{P}_i=\alpha_i\boldsymbol{E}_i. \tag{3}$$

$\boldsymbol{A}_{ik}$ is the 3×3 off-diagonal tensor of the interaction matrix,

$$\boldsymbol{A}_{ik}=\frac{\exp(\mathrm{i}kr_{ik})}{r_{ik}}[k^2(\boldsymbol{e}_{ik}\boldsymbol{e}_{ik}-\boldsymbol{1}_3)+\frac{\mathrm{i}kr_{ik}-1}{r_{ik}^2}(3\boldsymbol{e}_{ik}\boldsymbol{e}_{ik}-I_3)],$$

$$i\neq k, \tag{4}$$

where r_{ik} is the distance between r_i and r_k, $\boldsymbol{e}_{ik}$ is the unit direction vector from point r_i to r_k. From the Helmholtz equation we obtain $\boldsymbol{A}_{ik}=k^2\boldsymbol{G}_{ik}$, where $\boldsymbol{G}_{ik}$ is the Green's function of the electric field generated by the radiating dipole r_i. Defining $\boldsymbol{A}_{ii}=\alpha_i^{-1}$, substituting it into Eq.(2), we obtain:

$$\sum\nolimits_{k=i}^{N}\boldsymbol{A}_{ik}\boldsymbol{P}_i=\boldsymbol{E}_{\mathrm{inc},i}\ . \tag{5}$$

However, placing the nanoparticles in the vicinity of a surface, the surface reflection is unneglectable. In the presence of the surface, it is necessary to consider the reflection effect between 'image' dipoles on the surface of the substrate. The incident field should be the sum of the two effects, the expression of incident field is given by:

$$\boldsymbol{E}_{\mathrm{inc},i}=\sum\nolimits_{k=1}^{N}\boldsymbol{A}_{ik}^{SI}\boldsymbol{P}_i=\sum\nolimits_{k=1}^{N}(\boldsymbol{A}_{ik}+\boldsymbol{R}_{ik})\boldsymbol{P}_i\ , \tag{6}$$

where $\boldsymbol{R}_{ik}$ is an additional term of surface reflection. The specific formulation is given as[20]

$$\boldsymbol{R}_{ik}=\begin{bmatrix}\hat{r}_{ikx}^{I2}I_\rho^H-\hat{r}_{iky}^{I2}I_\phi^H & \hat{r}_{ikx}^{I2}\hat{r}_{iky}^{I2}(I_\rho^H+I_\phi^H) & \hat{r}_{ikx}^{I2}I_\rho^V\\ \hat{r}_{ikx}^{I2}\hat{r}_{iky}^{I2}(I_\rho^H+I_\phi^H) & \hat{r}_{ikx}^{I2}I_\rho^H-\hat{r}_{iky}^{I2}I_\phi^H & \hat{r}_{iky}^{I2}I_\rho^V\\ -\hat{r}_{ikx}^{I2}I_\rho^V & -\hat{r}_{iky}^{I2}I_\rho^V & I_z^V\end{bmatrix}-$$
$$\frac{k_1^2-k_2^2}{k_1^2+k_2^2}\frac{\exp(\mathrm{i}k_0r_{I,ik})}{r_{I,ik}}\times$$
$$\begin{bmatrix}-(\beta_{ik}^I+\gamma_{ik}^I\hat{r}_{ikx}^{I2}) & -\gamma_{ik}^I\hat{r}_{ikx}^{I2}\hat{r}_{iky}^{I2} & \gamma_{ik}^I\hat{r}_{ikx}^{I2}\hat{r}_{ikz}^{I2}\\ -\gamma_{ik}^I\hat{r}_{iky}^{I2}\hat{r}_{ikx}^{I2} & -(\beta_{ik}^I+\gamma_{ik}^I\hat{r}_{iky}^{I2}) & \gamma_{ik}^I\hat{r}_{iky}^{I2}\hat{r}_{ikz}^{I2}\\ -\gamma_{ik}^I\hat{r}_{ikz}^{I2}\hat{r}_{ikx}^{I2} & -\gamma_{ik}^I\hat{r}_{ikz}^{I2}\hat{r}_{iky}^{I2} & \beta_{ik}^I+\gamma_{ik}^I\hat{r}_{ikz}^{I2}\end{bmatrix}, \tag{7}$$

$$\hat{r}_{ikx,y,z}^I=\frac{\hat{r}_{ikx,y,z}^I}{r_{ik}^I}\ , \tag{8}$$

$$r_{ik}^I=\sqrt{(x_i-x_k)^2+(y_i-y_k)^2+(z_i-z_k)^2}\ , \tag{9}$$

$$\beta_{ik}^I=[\boldsymbol{1}-(k_0r_{ik}^I)^{-2}+\mathrm{i}(k_0r_{ik}^I)^{-1}], \tag{10}$$

$$\gamma_{ik}^I=-[\boldsymbol{1}-3(k_0r_{ik}^I)^{-2}+3\mathrm{i}(k_0r_{ik}^I)^{-1}], \tag{11}$$

where I_ρ^V, I_ϕ^H, and I_z^V are the Sommerfeld identities[1]. Defining higher refractive index n_1, lower refractive index n_2, incident angle θ_1 and transmitted angle θ_2, the wave vector of the evanescent field is given by

$$\boldsymbol{k}_e=(0,\ n_2k_0\sin\theta_2,\ n_2k_0\cos\theta_2), \tag{12}$$

$$\sin\theta_2=(n_2/n_1)\sin\theta_1\ , \tag{13}$$

$$\cos\theta_2=\mathrm{i}\sqrt{(n_2/n_1)^2\sin^2\theta_1-1}\ . \tag{14}$$

Thus, the unit direction vectors of TM and TE wave are given by:

$$\boldsymbol{e}_p=(0,\mathrm{i}\sqrt{(n_2/n_1)^2\sin^2\theta_1-1},(n_2/n_1)\sin\theta_1)\ ,$$
$$\boldsymbol{e}_s=(1,0,0)\ . \tag{15}$$

The corresponding Fresnel formulas of *s*- and *p*-polarization will be:

$$T_{e,p}=\frac{2n_1\cos\theta_1}{n_1\cos\theta_1+(n_2/n_1)\sqrt{n_2^2-n_1^2\sin^2\theta_1}}\left|E_{1,p}\right|, \tag{16}$$

$$T_{e,s}=\frac{2n_1\cos\theta_1}{n_1\cos\theta_1+\sqrt{n_2^2-n_1^2\sin^2\theta_1}}\left|E_{1,s}\right|\ . \tag{17}$$

The corresponding evanescent field in the surface of medium will be given by:

$$\boldsymbol{E}_{e,p}=\boldsymbol{e}_p|T_{2,p}|, \tag{18}$$

$$\boldsymbol{E}_{e,s}=\boldsymbol{e}_s|T_{2,s}|. \tag{19}$$

In our model, the dipoles are illuminated by the evanescent wave that generated by the plane wave undergoing total internal reflection. Eqs.(18) and (19) describe the evanescent wave fields of vertical and parallel polarization, respectively. Then the field of nanoparticles is calculated by Eq.(6)[26].

Another physical quantity to be studied in the article is the extinction coefficient, and the extinction cross section is defined as

$$C_{\mathrm{ext}}=\frac{4\pi k}{\left|\boldsymbol{E}_0\right|^2}\sum\nolimits_{i=1}^{N}\mathrm{Im}\left(\boldsymbol{E}_{\mathrm{inc},i}^*\cdot\boldsymbol{P}_i\right). \tag{20}$$

The extinction coefficient is the extinction cross section divided by the cross-sectional area of the scatterer[27].

In this work, the scattering object is ANPs with a diameter of 30 nm, the range of wavelength is from 300 nm to 700 nm. The refractive index of the substrate (BK7 glass) is 1.15—1.55[28]. Thus, the critical angle is about 40°—42°. An incident angle of 45° is thus selected to ensure the total internal reflection. In previous studies, the probe of the atomic force microscope (AFM) is represented as an array of dipoles and analyzed the change of dipoles field intensity when the distance between the probe and the nanoparticle changes. Taking the spacing of 1 nm and 14 nm as examples, closer distance between the probe and the nanoparticles provides higher field enhancement[1,20,29]. We thus varied the separation distance of nanoparticles by changing the coordinates of each discretized nanoparticle. l_1 (10 nm<l_1<15 nm) and l_2 (0<l_2<1 nm) to two cases of nanoparticles distributions, respectively. In every case, the separation distance of nanoparticles is limited between the minimum and maximum of l. Fig.1 shows the selected field intensity distributions of nanoparticles at separation l_2.

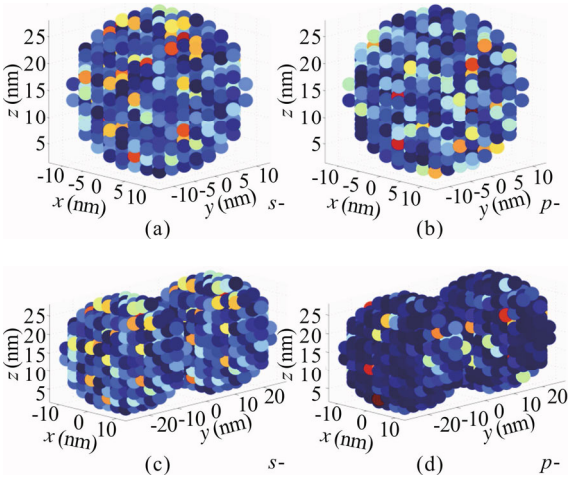

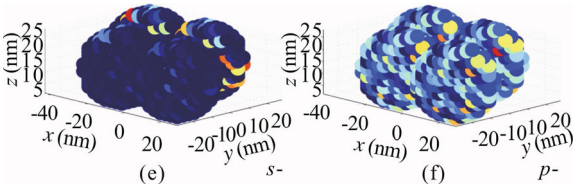

Fig.1 The field intensity distribution of each dipole in the case of incident plane waves with different polarizations: (a) and (b) are the case of one ANP is placed on the substrate; (c) and (d) are the case of two ANPs are placed on the substrate; (e) and (f) are the case of four ANPs are placed on the substrate

We took the mean of the field intensity of 552 dipoles as the field intensity of each nanoparticle. Changing the wavelength of the incident wave and the number of nanoparticles, the variation of the field intensity of nanoparticles is shown in Fig.2.

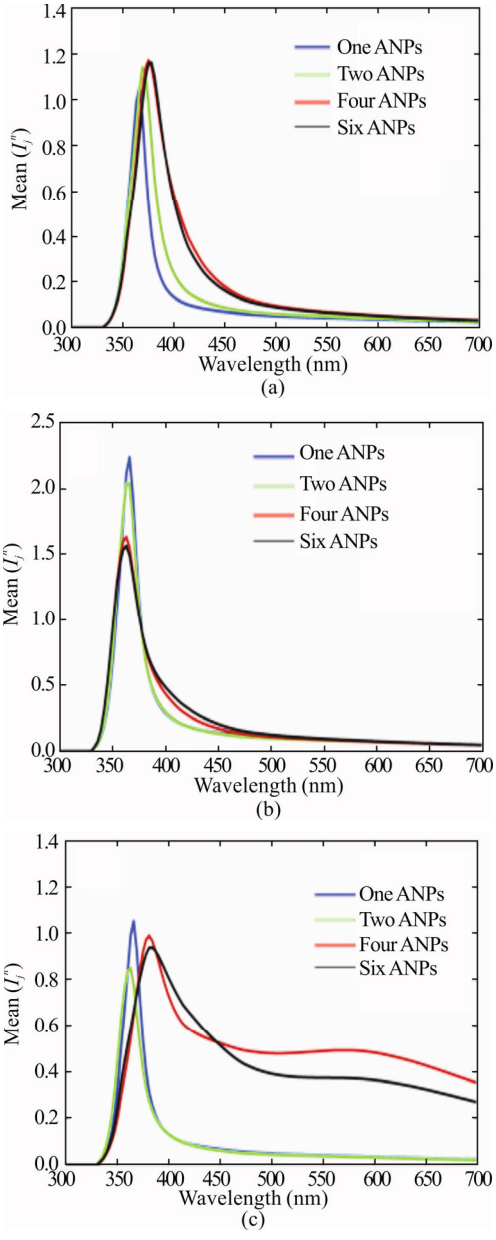

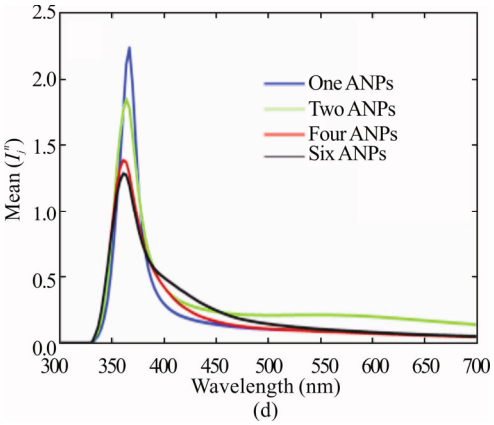

Fig.2 The field intensity of nanoparticles versus the incident wavelength: (a) and (b) The separation of nanoparticles is l_1; (c) and (d) The separation of nanoparticles is l_2; (a) and (c) Scattering object is illuminated by *s*-polarization wave; (b) and (d) Scattering object is illuminated by *p*-polarization wave

It is worth noting that the field intensities of different numbers of nanoparticles are significantly different at the same wavelength. Compared with *s*-polarization, *p*-polarization illumination provides higher field enhancement. The reason for this phenomenon is that although all the nanoparticles are placed in the same horizontal plane, the lateral coupling between the nanoparticles is dominant. The TM field consists of lateral and vertical components, whereas the TE field is completely a lateral component. In Fig.2(c), when the nanoparticles are illuminated by *s*-polarization wave and the wavelength of incident wave exceeds 400 nm, four and six nanoparticles have higher field enhancement compared to the case where the distance between the nanoparticles is l_1, in Fig.2(a).

As shown in Fig.3, different numbers of nanoparticles introduce a significant peak shift of the extinction efficiency at the same incident wavelength. In Fig.3(a) and (b), the nanoparticles are illuminated by different polarization waves, the peak shift is completely in different direction. It is the same in Fig.3(c) and (d).

From Fig.3, we can conclude that when the external conditions are consistent, the more the number of nanoparticles, the smaller the value of the extinction efficiency. After changing the polarization direction of the incident wave and the spacing between the nanoparticles, the change of extinction efficiency of multiple nanoparticle system is more obvious than that of a single nanoparticle system. The number of nanoparticles and the distance between nanoparticles change the near-field coupling effect of the nanoparticles, it redistributes the surface electrons between the surface and the volume, resulting in the appearance of the above two phenomena.

The size of the nanoparticle is also an important factor that cannot be ignored in practical applications[30]. In Fig.4, the field enhancement changes for different size nanoparticles. In order to eliminate the influence of the wavelength on the simulation results, we used the same incident wave at 632.8 nm.

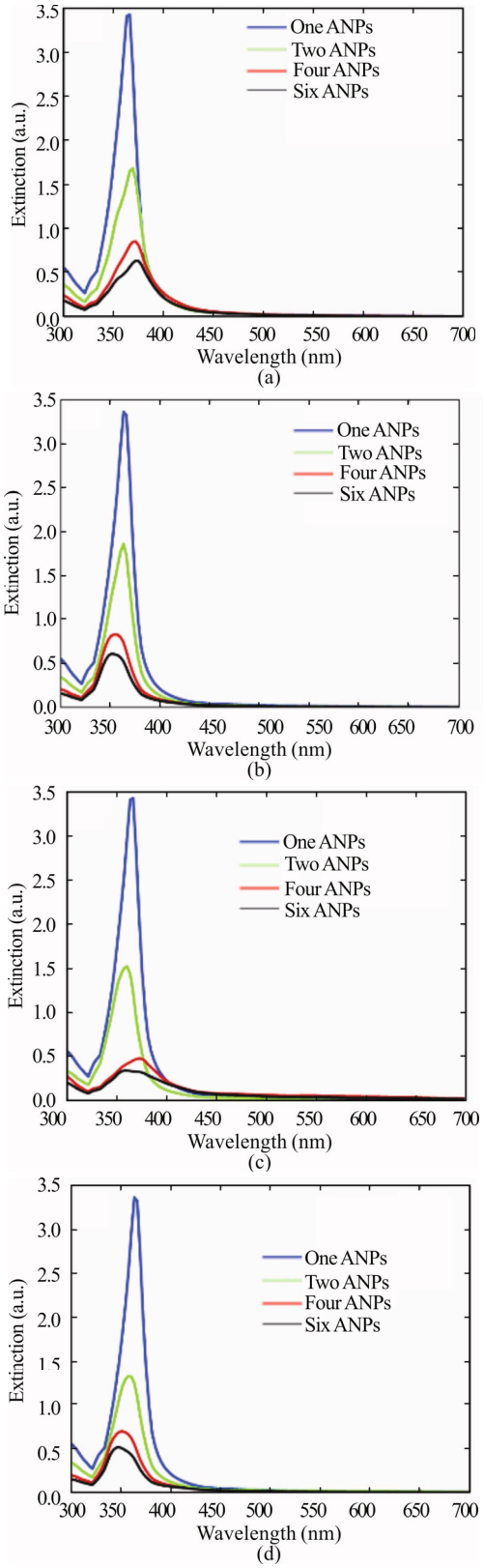

Fig.3 The extinction efficiency of nanoparticles versus the incident wavelength: (a) and (b) The separation of nanoparticles is l_1; (c) and (d) The separation of nanoparticles is l_2; (a) and (c) Nanoparticles are illuminated by *s*-polarization wave; (b) and (d) Nanoparticles are illuminated by *p*-polarization wave

As shown in Fig.4, the abscissa represents the diameter of each nanoparticle, the ordinate represents the field enhancement, and the curves of different colors are the different numbers of nanoparticles. We found that the field enhancement not only changes with the number of nanoparticles, but also with the diameter of the nanoparticles. In terms of the magnitude of the field enhancement, it is similar to the results obtained in Fig.2, that is, the field enhancement around the nanoparticles is more obvious under *p*-polarization. The lateral coupling between the nanoparticles is dominant. Overall, the field enhancement is proportional to the number of nanoparticles, both in the case of *s*-polarization and *p*-polarization, but additionally the larger number of nanoparticles brings larger diameter of the nanoparticles at the peak position to achieve the maximum field enhancement.

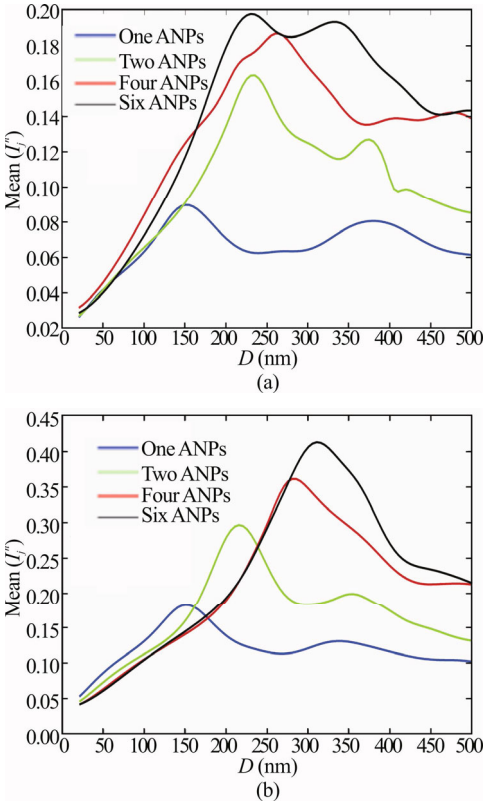

Fig.4 The field intensity of nanoparticles versus the diameter (*D*) of the nanoparticles (The separation of nanoparticles is l_2): (a) Scattering object is illuminated by *s*-polarization wave; (b) Scattering object is illuminated by *p*-polarization wave

In summary, we have exploited the DDA method to simulate a multi-nanoparticle system. By varying the number of nanoparticles, the spacing of multiples nanoparticles, the incident wavelength, we studied the field enhancement and the extinction efficiency of multiple nanoparticles. This developed DDA algorithm provides a method to perform analysis of near filed coupling in the multiple-nanoparticles system. Our work may improve the use of

multiple-nanoparticles in the field of catalysts, optics, and biosensing.

References

[1] V. L. Y. Loke and M. P. Menguc, Journal of the Optical Society of America a-Optics Image Science and Vision **27**, 2293 (2010).

[2] T. W. H. Oates and A. Mucklich, Nanotechnology **16**, 2606 (2005).

[3] K. A. Willets and R. P. Van Duyne, Annual Review of Physical Chemistry **58**, 267 (2007).

[4] S. S. Acimovic, M. P. Kreuzer, M. U. Gonzalez and R. Quidant, Acs Nano **3**, 1231 (2009).

[5] A. Bansal and S. S. Verma, Aip Advances **4**, 14 (2014).

[6] V. Amendola, R. Pilot, M. Frasconi, O. M. Marago and M. A. Iati, Journal of Physics-Condensed Matter **29**, 48 (2017).

[7] J. H. Yoon, F. Selbach, L. Langolf and S. Schlucker, Small **14**, 5 (2018).

[8] H.-y. Zhang, S.-g. Yu and M.-j. Bian, Optoelectronics Letters **14**, 241 (2018).

[9] I. D. Mayergoyz, Physica B-Condensed Matter **407**, 1307 (2012).

[10] J. F. L. Santos, M. J. L. Santos, A. Thesing, F. Tavares, J. Griep and M. R. F. Rodrigues, Quimica Nova **39**, 1098 (2016).

[11] V. Amendola, Physical Chemistry Chemical Physics **18**, 2230 (2016).

[12] J.-j. Wang and Z.-h. Jia, Optoelectronics Letters **15**, 439 (2019).

[13] T. Karakouz, A. B. Tesler, T. A. Bendikov, A. Vaskevich and I. Rubinstein, Advanced Materials **20**, 3893 (2008).

[14] K. A. Willets, A. J. Wilson, V. Sundaresan and P. B. Joshi, Chemical Reviews **117**, 7538 (2017).

[15] J. A. Scholl, A. Garcia-Etxarri, A. L. Koh and J. A. Dionne, Nano Letters **13**, 564 (2013).

[16] S. Kadkhodazadeh, J. R. de Lasson, M. Beleggia, H. Kneipp, J. B. Wagner and K. Kneipp, Journal of Physical Chemistry C **118**, 5478 (2014).

[17] S. Lerch and B. M. Reinhard, Nature Communications **9**, 1608 (2018).

[18] K. H. Su, Q. H. Wei, X. Zhang, J. J. Mock, D. R. Smith and S. Schultz, Nano Letters **3**, 1087 (2003).

[19] E. R. Encina and E. A. Coronado, Journal of Physical Chemistry C **114**, 3918 (2010).

[20] Y. Ruan, K. Li, Q. Lin and T. Zhang, Chinese Physics Letters **35**, 4 (2018).

[21] B. T. Draine and P. J. Flatau, Journal of the Optical Society of America a-Optics Image Science and Vision **11**, 1491 (1994).

[22] M. A. Yurkin and A. G. Hoekstra, Journal of Quantitative Spectroscopy & Radiative Transfer **106**, 558 (2007).

[23] M. A. Yurkin and A. G. Hoekstra, Journal of Quantitative Spectroscopy & Radiative Transfer **112**, 2234 (2011).

[24] O. A. Yeshchenko and A. O. Pinchuk, Reviews in Plasmonics 2017, C. D. Geddes, ed., Springer International Publishing, Cham, 285 (2019).

[25] B. T. Draine and J. Goodman, Astrophysical Journal **405**, 685 (1993).

[26] D. W. Mackowski, Journal of the Optical Society of America a-Optics Image Science and Vision **19**, 881 (2002).

[27] A. B. Evlyukhin, C. Reinhardt and B. N. Chichkov, Physical Review B **84**, 8 (2011).

[28] B. J. Frey, D. B. Leviton, T. J. Madison, Q. Gong and M. Tecza, Cryogenic Optical Systems and Instruments Xii, J. B. Heaney and L. G. Burriesci, ed., Spie-Int Soc. Optical Engineering, Bellingham, 2007.

[29] W. Y. Rao, Q. Li, Y. Z. Wang, T. Li and L. J. Wu, Acs Nano **9**, 2783 (2015).

[30] C. Jing, Z. Gu, Y. L. Ying, D. W. Li, L. Zhang and Y. T. Long, Analytical Chemistry **84**, 4284 (2012).